LHCb/98-066 RICH
2nd February 1999

EVALUATION OF THE MULTI-ANODE PHOTOMULTIPLIER FOR THE LHCb RICH DETECTORS

N. Smale, J. Bibby, N. Harnew and S. Topp-Jorgensen

University of Oxford

ABSTRACT

This report describes laboratory tests of the 64-pixel R5900-00-M64 Hamamatsu Multi-Anode Photomultiplier tube, under study for the LHCb RICH detectors. Results are presented on pixel gain uniformity, active area, relative efficiency and single photon resolution.

1) INTRODUCTION

Hybrid Photodiodes (HPD's) have been proposed for the LHCb RICH detectors as a baseline option [1]. However Multi-Anode Photomultiplier tubes (MAPMT's), which have now been operated successfully in the HERA-B RICH detector, could be a second viable solution. The MAPMT has excellent signal-to-noise properties, and offers ~200 times the gain of the HPD for running voltages less than 1 kV. It is therefore less demanding on the front-end readout electronics. In its favour, the HPD potentially offers the advantage of a much larger surface area per tube, hence alleviating the need for a lens system when close-packing the devices. In addition the HPD has considerably better single photon resolution. The final choice of device for the LHCb RICH system will depend on advances in HPD design, readout, cost and availability.

In order to make a reasonable assessment of the properties of the MAPMT and to ensure the suitability of the tube for the LHCb physics application, a 64-pixel device has been studied on a photon scanning facility in Oxford. Photons from a light spot of 420nm wavelength and 47μm in diameter have been scanned across the surface of the MAPMT tube in 100μm steps. Results from these scans are presented in this note.

2) THE MULTI-ANODE PHOTOMULTIPLIER TUBE

The photomultiplier tube under investigation is the R5900-00-M64 MAPMT from Hamamatsu, shown in Fig. 1. Its physical dimension is $30mm^2$ x 50mm (including external housing). The detection area of the tube is an 800μm thick borosilicate window with an

18.1mm^2 bialkali photocathode that has a peak wavelength response of 420nm. Photoelectrons are electrostatically focussed onto an array of 8 x 8 metal channel dynode stages, each stage having 12 dynodes (bialkali on stainless steel) [2]. This effectively gives 64 pixels, each with a 2mm^2 detection area. Each pixel has its own anode pin. The tube has a quantum efficiency of ~20%, and the gaps between pixels are approximately 300μm.

The MAPMT anode was terminated with a 50Ω load. With a bias voltage of -1000V the gain is about 1x10^6, and output signals typically have rise times of 1.5ns with 5ns duration [2]. For a single photoelectron with charge 1.6x10^{-19}C, a 2mV signal is expected at the load. The gain can vary between pixels by a factor of 5. However the variation does not follow a normal distribution, rather the large gain variation is dominated by a few 'bad' pixels, typically 5% of the tube.

For the purposes of the studies described below, eight of the anode signals are simultaneously read out into a NIMS module 16 channel amplifier, model 776, each channel having a gain of 100. The amplified signals are ac-coupled to a CAMAC 12 channel ADC, model 2249A. Capacitors are necessary to remove the dc offsets of the amplifiers.

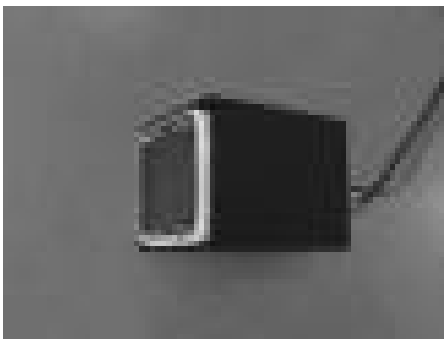

Fig. 1 : Photograph of a MAPMT. The physical size is 30mm^2 x 50mm.

3) THE LIGHT SCANNING FACILITY

The following subsections give details of the set-up required to deliver photons using an LED via fibre optics, and the system for scanning the light source across the MAPMT.

3.1) MECHANICAL HOUSING AND MOUNTING

In order to protect the MAMPMT from extraneous light, a dark box housing of 0.75x0.4x0.16m (L,W,H) has been constructed, a schematic of which is shown in Fig. 2. All feedthrough connectors are electrically isolated from the box by nylon washers to reduce ground loops. Anodes 1 to 64 of the MAPMT are read out via individual coaxial cables with LEMO connectors, with a common ground point on the tube. The MAPMT is supported and clamped using a silicon resin bonded fibre (SRBF) block. This is used for its insulation properties since the inner case of the MAPMT is held at bias potential to prevent current leakage across the window. Foam inserts are used to prevent damage to the tube.

3.2) LED LIGHT SOURCE AND OPTICAL COUPLING

The peak response of the MAPMT is 420nm (blue light). It would have been advantageous to use coherent light of the type produced by a laser, suitable for coupling to monomode fibres. This could have been focussed to a much smaller spot than incoherent light produced by a LED. Unfortunately blue lasers are expensive so a blue 470nm LED was used, with a maximum luminosity of 1000 milli candela and a view angle of 15 degrees, switched at 10kHz with pulse duration of 15ns. The short duration was required so that ADC gating could be minimised to reduce capture of MAPMT dark counts and system noise. An electronic circuit was constructed with FET gates so that the LED cathode was held at bias voltage until switched on, another FET was used to switch the LED off, shown in simplified form in Fig. 3. The LED was mounted outside the light box (electrical switching noise would have resulted had it been mounted inside). To deliver the LED light pulse to the MAPMT window a monomode fibre was used. This was for two reasons: 1) to restrict the pulse to a narrow light spectrum with spot size conforming to a Gaussian distribution, 2) to minimise the spot size from the end of the fibre by reducing aberrations. This is explained in section 3.3.

The first step in coupling an LED to a monomode fibre is to use an objective lens to form a parallel beam. This proved difficult as the LED has its own encapsulated lens and is an incoherent light source. The parallel beam is then focussed through a second objective lens to a spot size that matches the fibre. In practice the spot was 1mm in diameter. A local x,y,z stage is used to align the fibre with the focussed light spot, shown in Fig. 2.

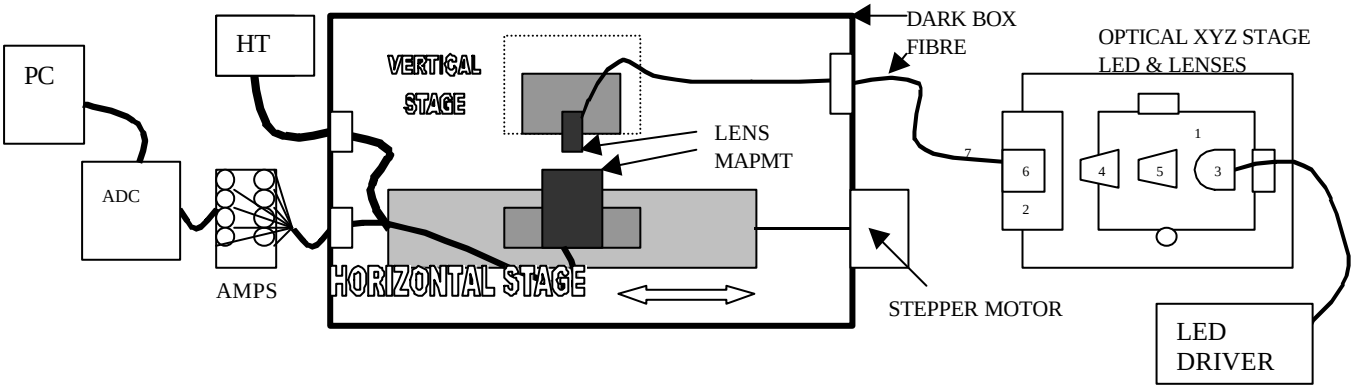

Fig. 2 : The test setup. 1) Optical x,y,z stage 200nm resolution, 2) A large fixed platform for mounting lenses, 3) Blue LED, 4) times 10 objective lens, 5) times 20 objective lens, 6) FC receptacle to except fibre, 7) Monomode fibre core diameter 3.5µm, cladding 125µm, numerical aperture (NA) 0.11 with a graded index lens on the end with focal length of 25mm, diameter 3mm.

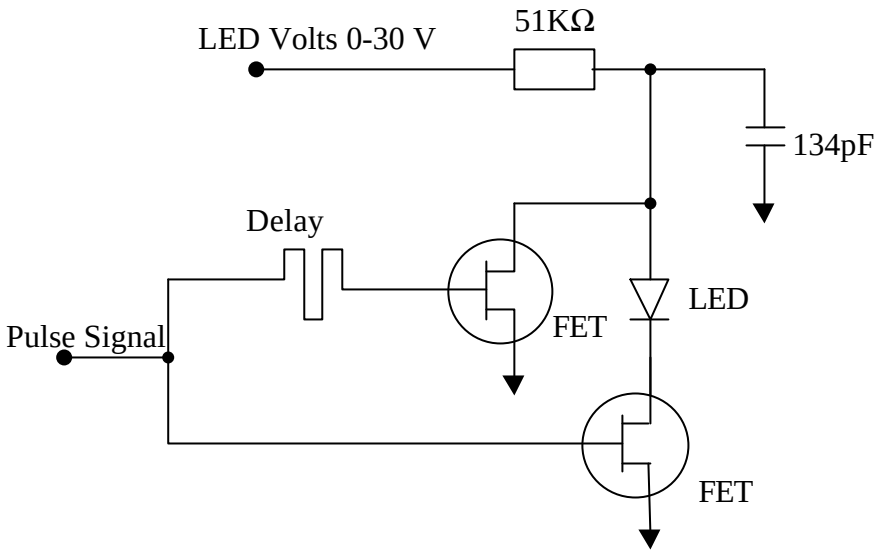

Fig. 3 : The basic FET circuit for pulsing the LED.

3.3) MONOMODE FIBRE AND LIGHT SPOT SIZE

A monomode fibre with core diameter 3.5 μm was used throughout these studies. A light wave entering the fibre is either refracted into the cladding, and attenuated, or is totally internally reflected at the core/cladding boundary. In this manner it travels along the length of the fibre. There are actually only certain 'allowed' incident angles, θ_{accept} , that will propagate through the fibre and these define the modes of the waveguide. The number of modes in a given waveguide depends on the optical frequency being transmitted and can be estimated from the normalised frequency or V-number: $V= [2\pi\ r_{core}\ /\lambda]\ \sin\theta_{accept}$ and the number of modes is $N= V^2/2$. For V<2.405, N=2 the fibre is then termed a monomode [3]. The larger the value of acceptance angle, defined as the numerical aperture (NA), the larger the cone of light which can be coupled into the fibre and the more the light exiting the fibre will spread out. The fibre used for this project has NA=0.11. At the output of the fibre, due to the 800μm thick borosilicate window on the front of the MAPMT, the light spot would spread to a diameter of 200μm before being incident on the photocathode. Therefore, to obtain a more acceptable 47μm (FWHM) diameter, a graded index lens with a confocal parameter of $\sqrt{2}\ /\ 0.8mm$ was added to the end of the monomode fibre. This spot size was confirmed by using a CCD camera, the measured spot size distribution is shown in Fig. 4. The top of the distribution is missing as it overflowed the ADC range of the camera.

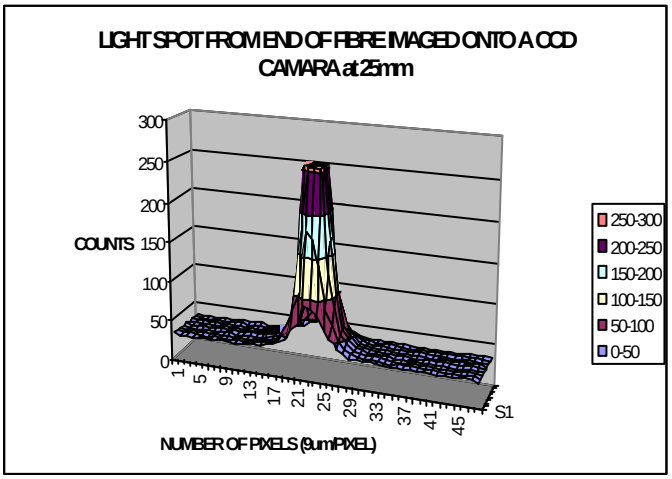

Fig. 4 : Light output profile from the end of the fibre, recorded by a CCD camera.

3.4) X-Y SCANNING STAGES

To enable scanning of the light across the face of the MAPMT, two motorised stages with 1μm resolution are used. One moves the MAPMT, the other moves the end of the fibre. A stepper motor driver unit that interfaces to a PC was designed and built to control the stages.

4) THE PERFORMANCE OF THE MAPMT

4.1) SINGLE PHOTON RESOLUTION

Although single photon resolution is not essential for LHCb RICH purposes, it may have some advantages [1]. The good single photon resolution of HPD's is well-known [4]; the single photon resolution of the MAPMT is presented here. The monomode fibre was positioned centrally on a MAPMT pixel. To select the working voltage of the LED to give single photons, the LED voltage (i.e the photon intensity) was increased from 6.0V to 30V in varying steps. For each setting the LED was triggered 100,000 times. No photons were detected below 6.1V. Fig. 5 shows four typical spectra, with the LED voltage at 11.3V, 13.1V, 16.0V and 19.0V. Fits were made to these spectra to determine the position of the single photon peak and the mean number of photons detected. The fits are shown in Fig. 5. The fitting procedure uses a Gaussian distribution to simulate the single-photon response of the MAPMT tube, and then sums Gaussians with widths increased by $\sqrt{N}$ for each additional N^{th} photon contribution. A Poisson distribution is used to constrain the probability for producing 0,1,2 etc. photons. A further Gaussian peak is added to fit the pedestal (ie. the zero photon peak). It can be seen that the fits to the data are excellent, showing in these four examples, mean numbers of photons of approximately 1, 1.5, 2 and 3, respectively. Although the multi-photon peaks are not resolved by the eye, the fits indicate that the photon response of the MAPMT tube is extremely well understood. Even though all parameters are allowed to vary freely, it can be seen that the fitted values for of the normalisation, sigma of the single photon peak, position of the single photon peak with respect to pedestal mean, and pedestal mean and sigma are unchanged – even though the shapes of the photon spectra are very different.

4.2) RELATIVE TUBE EFFICIENCY

Hamamatsu quotes the photocathode efficiency of the MAPMT to be 20% (an absolute measurement of which is more difficult and is not made in these studies). This gives no indication of the efficiency over the surface of the tube, such as between pixels. Any gap between pixels will reduce the local detection efficiency. To measure this effect, the entire tube was scanned in 100μm steps with the light source described in section 3.2. The LED voltage was set at 9V (to ensure single photons), and rows of eight pixels were read out in turn. The LED was triggered 10,000 times at each step. The signals received from the MAPMT above a 5 sigma noise cut (defined by dedicated pedestal runs) were classed as hits and counted. The total counts for each step is then plotted. An example of a scan is shown in Fig. 6. To find the relative tube efficiency an average of the counts over the flat top of the pixel (ignoring the dip in the centre of the pixel) was taken to represent 100% relative efficiency. This number was used to find the efficiency for all points integrated over the

surface of the tube. The relative efficiency for the entire tube is thus 77% ± 3% (which reduces to 71% ± 3% if the effect of 3 dead pixels is included).

The dead areas between pixels and inefficiencies at the centre of the pixels are clearly seen in Fig. 6. These effects are caused by the HT focusing wire geometry of the tube, seen below.

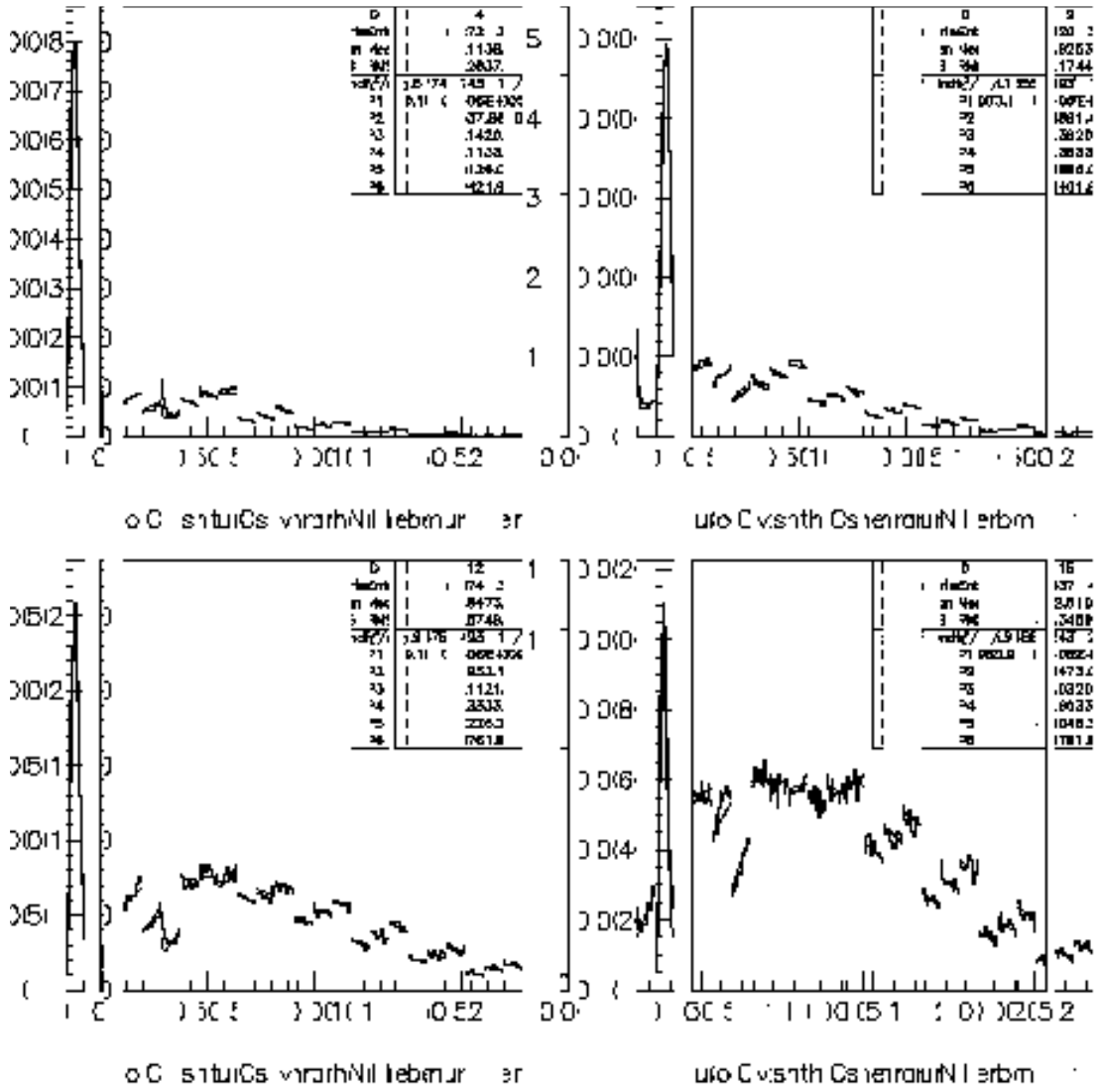

Fig. 5 : Fitted spectra in ADC counts (0.25pC/channel, bias voltage –950V), LED voltages as described in the text. The parameters are: P1 Normalisation; P2 Mean number of photons detected; P3 Sigma of the single photon peak; P4 Position of single photon peak with respect to the pedestal mean; P5 Pedestal mean; P6 Pedestal sigma.

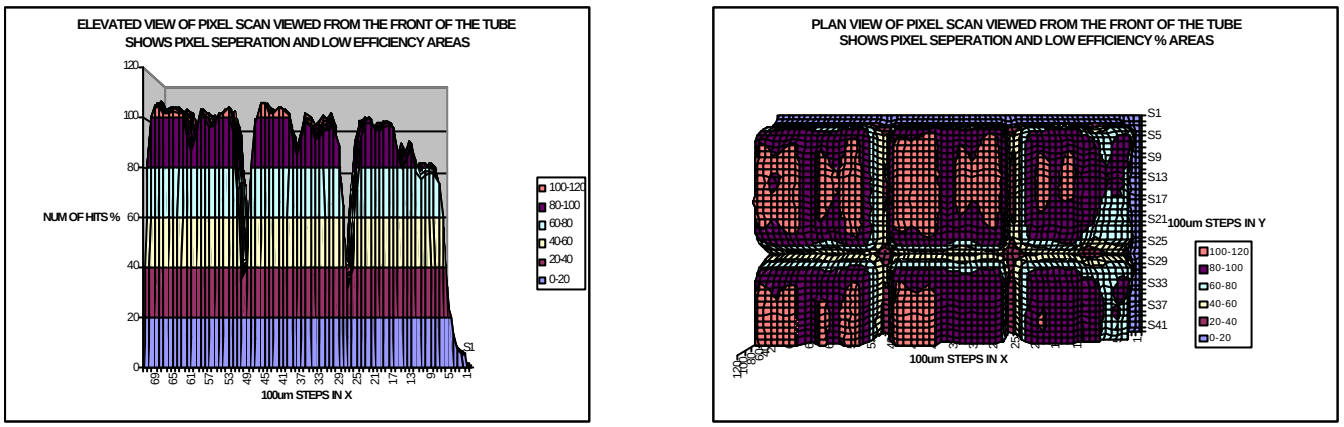

Fig. 6 : Examples of 1D and 2D scans across the face of the MAPMT pixels.

A photograph looking through the MAPMT window is shown in Fig. 7. This shows a single pixel, with two entries into the dynode chain. Around the pixel edge is a pair of focusing wires and through the middle of the pixel is a single focussing wire, slightly off centre, to optimise the focussing properties. This area defines the inefficient regions within a pixel, which were clearly observed in Fig. 6.

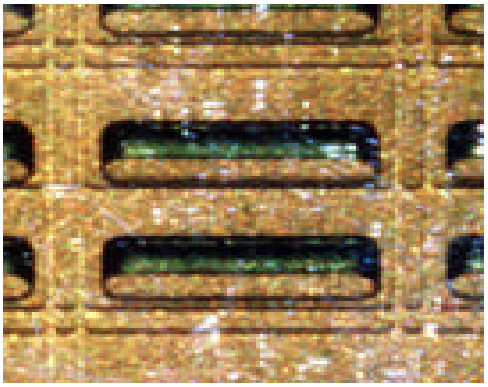

Fig. 7 : Photograph looking through the MAPMT window.

4.3) PIXEL GAIN UNIFORMITY

The variation of photoelectron gain, with the bias voltage at –950V, was studied at various locations of the tube. Pixel 13 (a central pixel) was measured in a 5x5 array of 300μm steps. At each step the LED was triggered 100,000 times, the signals from the MAPMT histogramed, and the single photon peak fitted (as in section 4.1). The resulting variation of gain over the pixel was found to have an RMS of 15±5% of the mean value. The light source was then scanned over the centre of each pixel and similar single photoelectron spectra measurements taken. The distribution of the mean of the single photon peak is shown for the 64 pixels in Fig. 8. The spread of the histogram gives the gain uniformity for single photon response. Although the gain uniformity is generally good, there are certain channels with relatively low gain response, as specified by Hamamatsu [2]. If the five pixels with low gain are ignored the gain variation is less than 20% RMS.

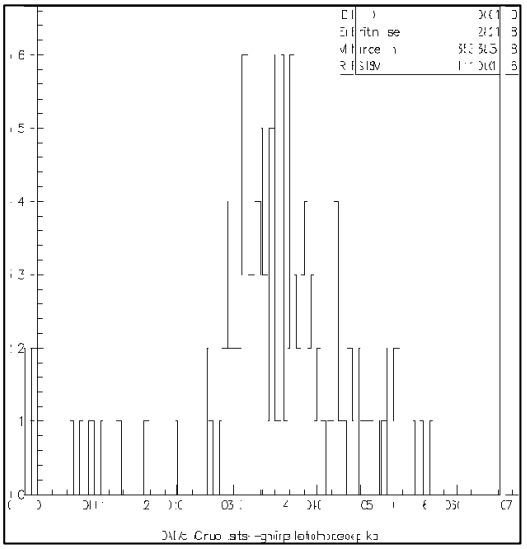

Fig. 8 : Distribution of the mean of the single photon peaks in ADC counts, for 64 pixels.

5) CONCLUSIONS AND REMARKS

The 64-pixel R5900-00-M64 MAPMT has been tested on a light-scanning facility in Oxford. The MAPMT performs largely to Hamamatsu's specifications by way of gain, uniformity, and single photon resolution. The single photon resolution (section 4.1) is very poor compared to the HPD. Both the HPD and the MAPMT have in principle the same quantum efficiency, however due to the focussing and gain structure of the MAPMT, these tests have shown the efficiency is reduced by ~23% with respect to the HPD (section 4.2). In addition to this, due to the inactive region around the MAPMT edges, a lens system would have to be utilized for the LHCb RICH detectors. However, with a single photon gain of $1x10^6$ electrons compared to 5-6000 for the HPD, the MAPMT could offer great simplification and cost advantages for the readout electronics and the HV system. From these results presented here, we believe that the MAPMT is a promising contender for the LHCb RICH detectors, now that the cost is competitive. Future work will be to upgrade the electronics to simultaneously read out all of the anode pins at LHC speeds.

REFERENCES

[1] LHC-b Technical Proposal CERN/LHCC 98-4 LHCC/P4 20 Feb 98.
[2] Hamamatsu R5900-00-M64 data sheet Sept 1997.
[3] Satellite/optical and mobile communication systems, Brunel University.
[4] E.Albrecht et al., NIMA 411 (1999).